Temperature and spectral dependent analysis of photocurrent in a-Si:H single junction p-i-n solar cells

R. KAPLAN[*], B. KAPLAN
Department of Science and Mathematics Education, University of Mersin, Yenisehir Campus, 33000 Mersin, Turkey

Characterization of amorphous (a-) Si:H p-i-n thin film solar cells with different transparent-conductive-oxide (TCO) sheet resistance is described with focus on the spectral photoresponse measurements. Current density-voltage (J-V) characteristics under dark and light, fill factor, temperature-dependent current density and solar cell diode quality factor, bias-dependent integrated quantum efficiency (IQE) are investigated. Solar cell diode quality factor decreases with increasing temperatures for all devices with different TCO sheet resistances. There exists commonly a voltage-dependent photocurrent density collection which affects J-V characteristcs and IQE measurements. The voltage and light bias dependence of these measurements can be used to diagnose some specific losses. It is found that at reverse bias, the IQE is almost independent of bias light and applied voltages. However it strongly depends on both parameters for forward biases. There is no a big TCO sheet resistance effect on the solar cell performance at all temperatures mesured (220-400 K). The results are interpreted in the light of standard device models.

1. Introduction

Solar cells for terrestrial applications are expected to assume one of two main forms: (i) large-area thin film solar cells, (ii) concentrating systems using single crystal cells. In the thin film approach, reduction of cost is achieved by using smaller amounts of materials and inexpensive processing. In the concentrator system approach, the higher cost of the single crystal solar cell is compensated by the increased energy conversion efficiency under higher illumination intensity. In this article, we concentrate on the large-area thin film amorphous p-i-n silicon solar cells.

Although the processing of thin film solar cells is among the most difficult, these cells of two very important advantages for terrestrial applications: first, since the required thickness of the active absorber layer is on the order of several times the optical absorption length of the material, direct bandgap solar cells can be made very thin, usually a few microns thick, thus lowering the material cost; and secondly, thin film configuration lends itself to large area, continuous flow processing.

Thin film solar cells based on amorphous (a-) Si:H , first reported in the mid 1970s [1] have been under intense research because of their technical interests. Hydrogenated amorphous silicon a-Si:H is usually produced by glow discharge decomposition of silane (SiH_4). Investigations have shown that a substantial proportion of hydrogen is incorporated into the amorphous silicon. A-Si:H material has high optical absorption that permits true thin film (about 1 micron) devices; is low cost; can be easily adapted to a variety of process modification; and manufacturing has accumulated megawatt-size commercial experience.

The most common a-Si:H solar cell structure used is the p-i-n cell fabricated on a glass substrate [2]. This type of cell is usually fabricated by depositing a thin silicon dioxide buffer layer on a soda-lime-silicate glass and then depositing a layer of tin oxide. The tin oxide is often textured to promote light trapping over the visible wavelength range so that the cells appear dark.

One major concern with a-Si:H material is that all device quality a-Si:H solar cells exhibit light-induced degradation, often referred to as the Staebler-Wronski effect [3]. The recombination of photogenerated carriers as well as the trapping of holes can create metastable dangling-bond states near mid-gap, which reduce the diffusion length and increase the space charge density in the i-layer, both effects can reduce the solar cell performance. When exposed to extended periods of darkness, the pre-illumination state can be recovered. Increased light intensity aggravates the degradation; elevated temperatures in the darkness accelerates the recuperation.

Photoconductivity measurements provide a simple way of obtaining information about transport, loss, and recombination mechanisms in amorphous semiconductors. The study of photoconductivity in hydrogenated amorphous silicon (a-Si:H) p-i-n solar cell produced by glow discharge decomposition of silane (SiH_4) remains of interest in connection with developing and understanding of the electronic and optical properties. The dependence of photoconductivity on the type and density of defects, the

Fermi energy, the temperature, the doping and the photoexcitation intensity are stil subjects of basic interest.

Spectral photoresponse measurements can provide a considerable amount of qualitative and quantitative information on device configuration and material properties. In this work, we measured J-V characteristics under dark and light, the temperature dependence of photocurrent density, and the spectral photoresponse as a function of the applied voltage and bias light in a-Si:H p-i-n solar cells with the different TCO sheet resistances. The results were interpreted in the light of photoconductivity models exist.

2. Samples and experimental details

The substrates were textured SnO_2-coated glass made by AFG (PVTCO). Single junction a-Si p-i-n layers were deposited by PECVD at BP Solarex. The SnO_2 strip of width w~0.8 cm had an In-solder contact to the SnO_2 at one end, and 6 devices (labeled m=1-6) fabricated in a row. Device areas were 0.27 cm^2. L is the distance along the TCO from the Ag contact to the m-th device, and L/W is the number of squares of TCO. Typically 2 rows of 6

devices were analised on each piece to establish repeatability. Further detailed descriptions about solar cell devices used here were given elsewhere [4].

A schematic diagram of measurement system used is given in Fig. 1. The variation of photocurrent density with temperature was studied over the range 220 K to 400 K, using a tungsten halogen lamp of light intensity 1000 W/m^2. The spectral response of photocurrent density was investigated over the range 400 to 750 nm.

Quantum efficiency (QE) was measured using a chopped (71 Hz) monochromatic light. A tungsten source (ELH tungsten halogen lamp) and grating monochromator (Kratos 251) with 2 mm slit widths produced a beam with a 13 nm FWHM bandwidth. Measurement were computer controlled and used a lock-in amplifier (Stanford Research System, Model SR 830) technique to recover the signal. The monochromatic photon flux ranged from $(1-5) \times 10^{15}$ cm^{-2} sec^{-1} over the range of 400 to 750 nm. Both d.c. bias light (to simulate 1 sun illumination) and bias voltage (to change the magnitude of polarity of the field) could be applied to the device. Measurements were not corrected for reflection or transmission losses of the device. Because these losses are very small, and their effects on the results are negligible.
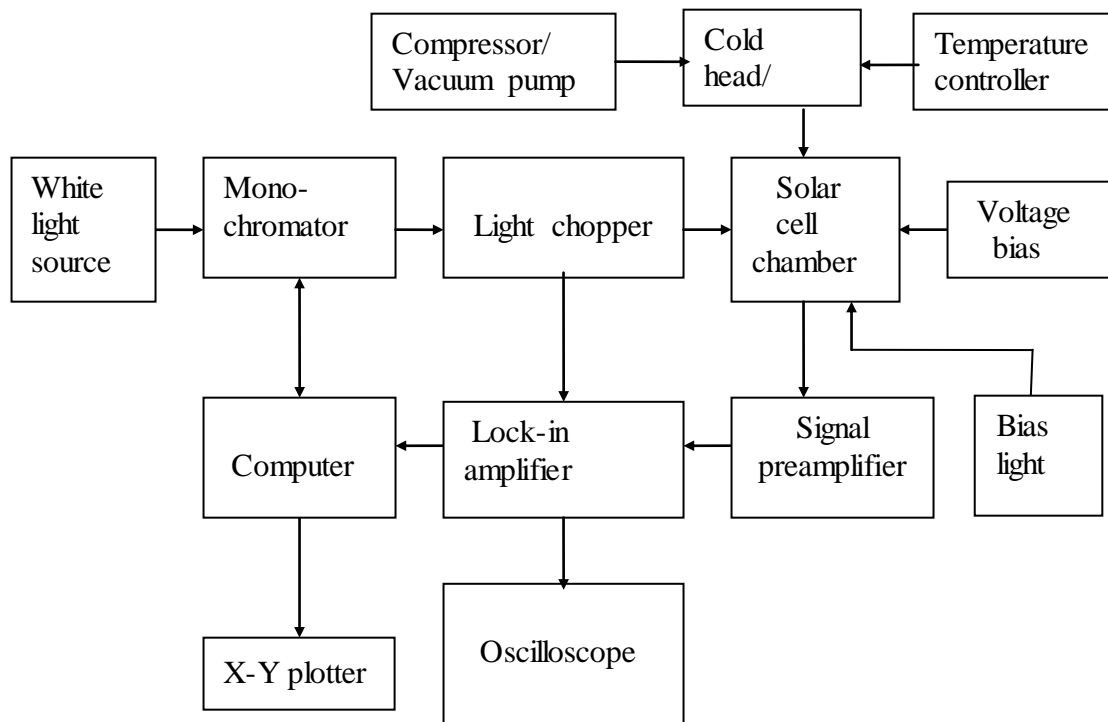

Fig. 1. Experimental set-up used

Before device measurements, a Laser Precision Corp. Model RS-5900 pyroelectric radiometer/detector is used to measure the spectral contents of the monochromatic beam, and this data, ranging from 400 nm to 750 nm in wavelength, is stored in computer for later calculation of quantum efficiency.

3. Results and discussion

Current density-voltage (J-V) measurements under standart illumination condition, 1000 W/m^2 (AM1.5) spectrum at room temperature, are the most common tool for solar cell investigation and characterization. The J-V plotting provides one to determinate the basic solar cell

parameters of the open-circuit voltage (V_{OC}), short-circuit current density (J_{SC}), fill factor (FF), and efficiency (η) which can be calculated by only three points on the J-V curve. While these parameters are well accepted indicators of solar cell performance and are particularly important for comparing and qualifying solar cells, there is a wealth of extra information that can be obtained by analyzing the entire J-V curve. This is particularly so if the current density dependence on light-intensity and temperature is considered [5-6].

In a thin film solar cell, the net external current density (J) through the device is the difference between the dark (J_D) and illuminated (J_L) current densities:

$$J = J_D - J_L. \qquad (1)$$

The dark current density-voltage, J-V, data can be analyzed with the following equations [7-8],

$$J_D (V) = J_o e^{q(V-JR_s)/AkT} \qquad (2)$$

$$J_o = J_R e^{-E_a/kT} \qquad (3)$$

where $V-JR_s$ is the voltage across the junction (i.e., across the i-layer), R_s is the series resistance, A is the diode quality factor, E_a is the activation energy, J_o is the diode current density, J_R is the prefactor, q is te fundamental electronic charge, k is the Boltzmann' constant, T is the temperature. The A, E_a and J_R are dependent on the specific recombination mechanism that dominates the forward current density J_o. And thus, the experimental determination of these solar cell diode parameters as a function of temperature and light intensity is fundemental.

In the dark, the circuit model for the total device consists of a junction diode in series with resistance. The total series resistance of the m-th device is the sum of the junction dynamic resistance R_J, the TCO/p contact resistance $R_{TCO/p}$, and the series resistance through the TCO R_{TCO}. R_{SH} is the sheet resistance of the TCO in Ω/sq. The derivative dV/dJ from Eqs.(1) and (2) yields (for $J_L \ll J_D$),

$$R = dV/dJ = R_J + R_{TCO/p} + R_{TCO} \qquad (4)$$

$$R_{TCO} = R_{SH} \times (L/W) \qquad (5)$$

$$R_J = (AkT/q) / J \qquad (6)$$

$$R_S = R_{TCO/p} + R_{TCO}. \qquad (7)$$

Each device in a given strip is assumed to have the same R_J and $R_{TCO/p}$. This has been verified experimentally. One term in Eq. (4) is inverse with J, and one is proportional to L/W. Plotting R vs 1/J will have an intercept of the series resistance R_S and slope AkT/q. Plotting R_S vs L/W will have an intercept of $R_{TCO/p}$ and a slope of R_{SH}. It was determined as $R_{SH}=14$ Ω/sq and $R_{TCO/p}=0.93$ Ω-cm^2 in detail elsewhere [9].

As well known, an ideal solar cell should have low series resistance and high shunt resistance in order to optimize the performance of device. The series resistance

includes a sum of several contributions. Especially, these may include spreading resistance through front or back electrodes, contact resistances, and through thin film resistance in the active absorber (intrinsic layer), or p-i interface layer in the solar cell. Various methods to seperate these contributions have been applied to thin film solar cells. Generally, this can be made by fabricating devices with systematically varied geometries or lateral current paths on a single substrate with all vertical device layers identical. Particularly, the device area can be varied to change the contact resistance contributions, and the lateral distance between devices and contacts can be varied to change the spreading resistance contributions [8]. Such a technique was used to compare devices with ZnO or SnO$_2$ contacts with the p-layer in a-Si:H p-i-n solar cells. The ZnO/p contact gave lower V_{OC} and FF, which was widely attributed to a barrier or contact resistance [10]. The shunt resistance is related to the loss of charge carriers due to current density leakage pathways and recombination of charges in the bulk or at the interfaces [11].

Fig. 2 shows J-V characteristics measured in dark (J_D) and under illumination (J_L) with white light for L/W=0.60 at room temperature (299 K). As seen, the current density under illumination gives rise to a FF value of 68.3 % with light illumination intensity of 1000 A/m^2 (AM 1.5). From the fourth quadrant in Fig. 2, the J_{SC}, defined as the current density during the external circuit without external applied voltage, and the open circuit voltage (V_{OC}) are determined to be 17.82 mA/cm^2 and 0.89 V, respectively. Although they are not shown here, similar results were also observed for other L/W values of 1.65, 4.12. 5.30, and 6.41. It is widely known that in a-Si:H p-i-n thin film solar cells, the V_{OC} is limited by built-in potential and dominated by bulk recombination at localizes states in the intrinsic (i-) layer or the recombination at the p/i interface [12,13]. The reason for low FF calculated can be attributed to the poor rectification property from the high reverse injection current which competes with the diffusion current under illumination apart from the lower excitation dissociation rate arising from the low charge carrier mobility in these cells.
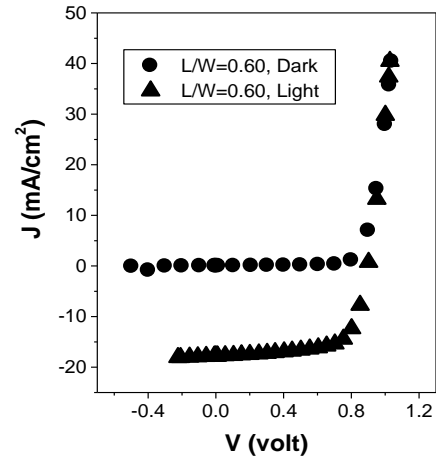

Fig. 2. Current density–voltage (J-V) characteristics of a-Si:H p-i-n solar cell in dark and under 1.5 AM illumination for L/W=0.6

It is important to talk about that sometimes in the literature, the voltage dependent current density collection is wrongly defined as a shunt loss. A true shunt is most clear as a linear increase in the dark current density at reverse bias where it should be negligibly small. However, as is obvious from Fig. 2, the dark curve is very flat and negligibly small at reverse bias exhibiting the absence of true shunt loss.

The basic diode behaviour and recombination mechanisms are the same for all thin film solar cells with different TCO sheet resistances. To illustrate this, it is helpful to look at the temperature dependence of J_o. Fig. 3 shows J_o as a function of 1/T for only the ratio of L/W=0.6 in the temperature range 220 to 400 K. As seen, the J_o decreases with decreasing temperature. It gives almost a straight line. Using Eq. (3), an average value of about $E_a =$ 0.52 eV was determined. This is also valid for all L/W ratios. Because, there is no any observed sheet resistance effect on J_o. This indicates that all m devices must have the same junction properties. As well known in the activated photocurrent-temperature region measured, the result depends on sample history, and in particular on the Fermi level positions [14]. The formation of free electron and hole pair is highly field and temperature-dependent process which is reflected in the reverse bias photocurrent behaviour.
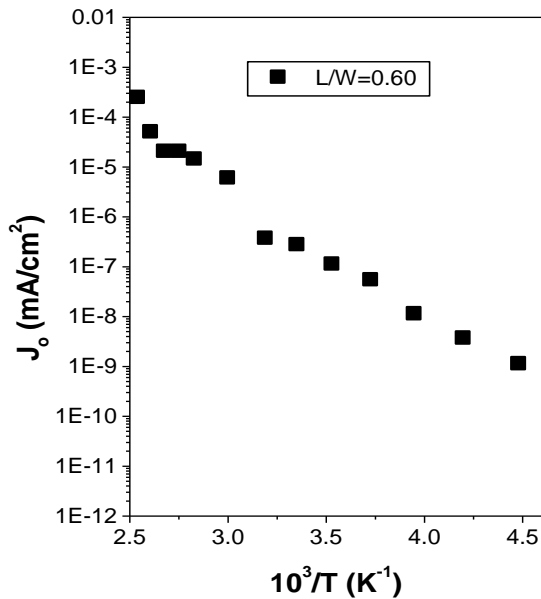

Fig. 3. J_o vs 1/T for L/W=0.6

Fig. 4 shows the variation of A-factor, which is the cell quality factor given by Eq.(2), with temperature for only L/W=0.6. As seen, A-factor decreases with increasing temperature to nearly 380 K. Again, we have observed that there is no L/W effect on A, due to uniformly deposition conditions. The A-factor is in the range 1.8-3.5 for all L/W values of 0.60, 1.65, 4.12. 5.30, and 6.41. This result together with E_a=0.52 eV indicate that the solar cell operates with the diode current density controlled by recombination through trap states in the

space-charge region of the intrinsic layer. The variation of A-factor between 1.8 and 3.5 depends on the energies of the deep defects that act as dominant trap states and its temperature dependence has been attributed to a distribution of traps or a tunneling contribution to the space-charge recombination current [8].
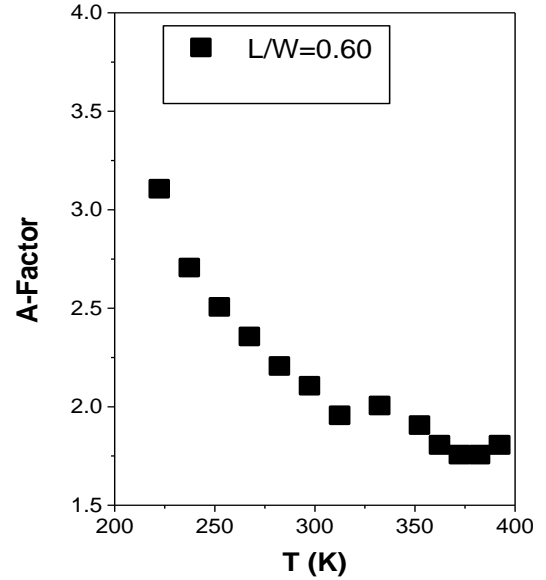

Fig. 4. Temperature dependence of A-factor for L/W=0.6

Quantum efficiency (QE) measurements in a-Si:H p-i-n solar cells are very important to characterize the photocurrent density and are commonly used to determine the losses responsible for reducing the measured J_{SC} from the maximum achievable photocurrent density. QE is a dimensionless parameter given by the number of electrons which exit the cell device per incident photon at each wavelength. The photocurrent densiy is the integral over wavelength of product of the measured external QE with the light spectrum, typically AM1.5 global for terrestrial solar cell devices. Thus a good verification of the QE mesurement is that the current density calculated by integrating the QE, measured with 0 V bias, with the AM1.5 spectrum agrees with J_{SC} [5].

The external quantum efficiency at a given wavelength is given by

$$QE(\lambda) = [J_{collec}(\lambda)/q] / \Gamma(\lambda) \qquad (8)$$

where q is the electronic charge, J_{collec} is the light-generated current density resulting from monochromatic illumination, and Γ is the incident photon flux given by

$$\Gamma = P (\lambda x 10^{-9}) / (h c) \qquad (9)$$

where P is the incident optical power density (in $J \cdot s^{-1} \cdot cm^{-2}$), λ is the wavelength (in nm), h is Planck's constant (in J-s), and c is the velocity of light (in $m \cdot s^{-1}$).

$J_{collec}(\lambda)$ is a complex function of several optical and electrical device parameters. Optical device parameters

include front- and back-surface reflectivity, optical distribution, absorption coefficient and total thickness. Electrical device parameters include front- and back-surface recombination velocity, emitter and base doping profiles, minority carrier diffusion length and emitter and base thicknesses.

The light-generated current density is calculated by integrating the product of the external quantum efficiency and the solar spectrum over wavelength

$$J_L = \int QE(\lambda)\ \Phi(\lambda)\ d\lambda \qquad (10)$$

where $\Phi(\lambda)$ is the solar spectrum expressed in mA/cm^2-µm. This calculation, as in our case, is commonly performed numerically.

Solar cell device losses measured by QE can be optical, because of the front reflection and absorption in the window, transparent conductor, and other layers, or electronic, because of recombination lossses in the absorber. Comparing the QE measured with different voltage bias is a strong tool to seperate electronic losses and optical losses since only the former should be affected by the applied bias voltage.

Spectral response measurements of solar cell devices can be made in dark, with light bias and/or voltage bias. Measurement data are stored on a disk for future reference. Figs. 5 (a) and (b) show the typical spectral response measurement results of a-Si:H p-i-n solar cell device under dark (no bias light) and light respectively for different reverse, zero and forward bias (voltage) conditions. As seen, the spectral response (from 400 to 750 nm) is qualitatively similar for different bias voltages. A peak is observed at a wavelength near 550 nm for all the biases measured. The integrated (calculated) quantum efficiencies (IQE) under spectral curves were also represented on the figures. Obviously, the value of IQE decreases with incresing forward bias conditions for both dark and light curves. However, under reverse bias, the IQE is almost constant, which shows that all carriers are collected without any electrical losses. Generally the IQE in a-Si:H p-i-n solar cells will increase with reverse bias.

As it is known, the IQE is dependent on the intrinsic layer's absorption coefficient α, thickness d, and an effective minority carrier collection length. It also depends on the external variables of the applied voltage, and bias light intensity. IQE decreases with increasing forward bias or increasing bias light intensity in a-Si:H p-i-n solar cell, due to a reduction in field and space charge width or due to series resistance effects including the TCO sheet resistance. At sufficient reverse bias (-1 V), the IQE reaches an optically limited maximum where there are no electronic losses, i.e., complete collection occurs, provided there is no light absorbed at the back contact. Optical enhancement, which commonly occurs in a-Si:H p-i-n solar cells due to light trapping, is included in IQE [15].
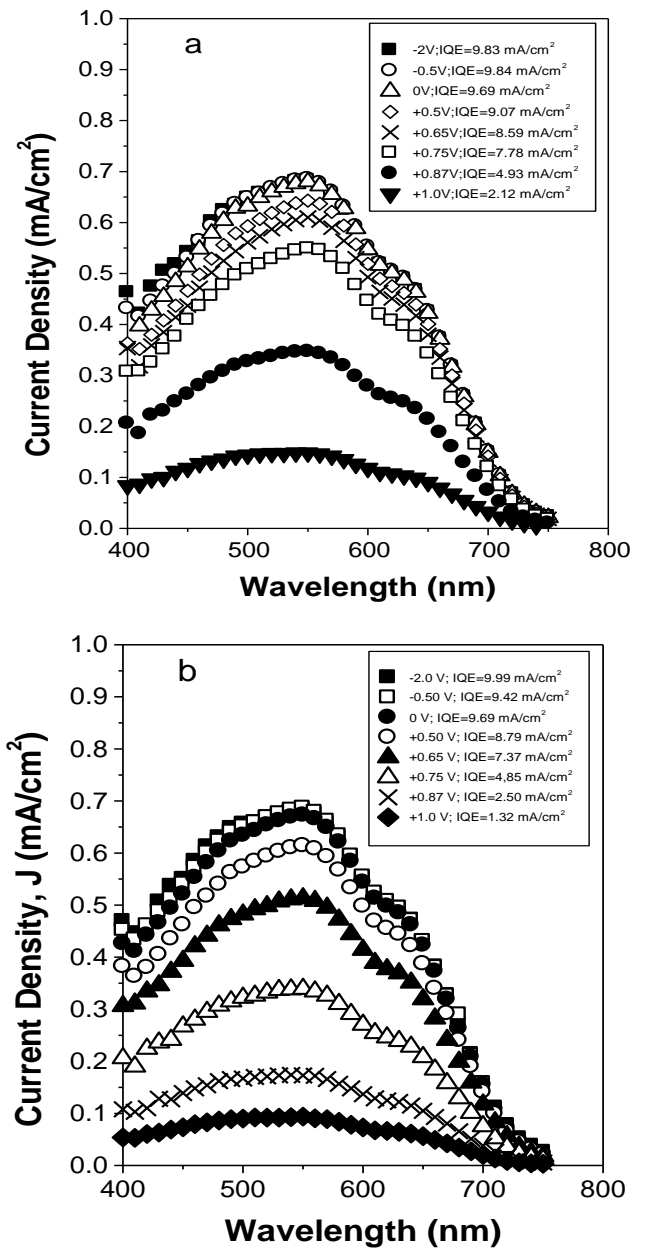

Fig. 5. Spectral photoresponse characteristics of the a-Si:H p-i-n cell under different applied bias voltages for with (a) and without (b) bias light conditions, respectively. (L/W = 0.6)

Fig. 6 shows the integrated quantum efficiency (IQE) as a function of applied bias voltage for with and without bias light. As seen, under the reverse bias the curves are almost constant and coincident, but under forward bias the IQE for both curves decreases sharply with increasing applied bias voltage and there is a small gap between them.
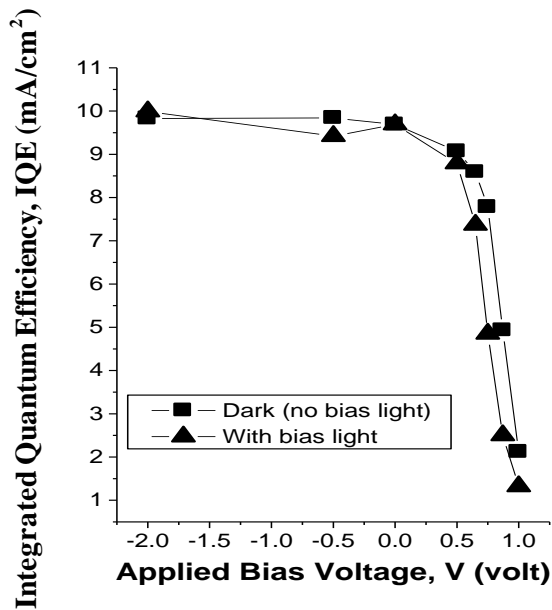
Fig. 6. A comparison of integrated quantum efficiency (IQE) vs applied bias voltage for with and without bias light. Lines are drawn as guides for the eye.(L/W = 0.6)

Standart J-V test conditions for solar cells usually use an illumination of ~1000 W/m^2. However, the monochromatic probe beam in a typical IQE measurement will be 3-4 orders of magnitude weaker. For idealized solar cells, these differences are not important, since the maesured response signals are assumed to be linear with input. The bias light will have negligible effect on solar cells with low trap density, but some thin film solar cells have nonlinear output because of trapping and photoconductivity [16]. The effect of white bias light on the IQE and collection in a-Si:H p-i-n solar cell is due to an increase in the positive space charge from trapped charge [17,18], which changes the applied electric field distribution and the regions with high or low drift-aided collection. The bias light effects can be even greater for IQE mesurements under red or blue bias light [18].

As well known, most of the incident light in a-Si:H p-i-n solar cell is absorbed in the intrinsic layer, generating the photocarriers which mostly contribute to the photocurrent. Light that is not absorbed in the intrinsic layer strikes the back contact where it is either absorbed and converted to heat or, partially reflected back into to intrinsic layer.

4. Conclusions

We present the temperature and spectral dependent analysis of a-Si:H single junction p-i-n solar cells. They have been fabricated with varying series resistance due to their TCO sheet resistance having a variable geometry aspect ratio L/W. Specially, we have obtained J-V characteristic under dark and light, temperature-dependent photocurrent density and quality factor, the voltage and light bias dependence of spectral photoresponse.

Under the light illumination intensity of 1000 A/m^2 (AM1.5), it was determined that V_{OC}=0.89 V, J_{sc}=17.82 mA/cm^2 and FF=68.3 % at room temperature for all L/W ratios. The temperature-dependent current density gives an activation energy value of about E_a=0.52 eV. The A-factor value was determined in the range 1.8-3.5 for all L/W (0.60 – 6.41) at temperatures 220-400 K. The variation of A-factor depends on the energies of the deep defects that act as dominant trap states and its temperature dependence has been attributed to a distribution of traps or a tunneling contribution to the space-charge recombination current. These results indicate that the solar cell operates with the diode current density controlled by recombination through trap states in the space-charge region of the intrinsic layer.

From the spectral dependence, in order to characterize the most relevant optical and collection effects with white bias light and in the dark, the integrated quantum efficiency (IQE) was determined as a function of bias voltage. At reverse bias, the IQE is found to be almost independent of the voltage and light bias. However it strongly depends on both parameters for forward biases. The voltage bias (due to the series resistance) caused by photocurrent density when the device is under illumination.

However we observed that there is no a big dependence of A, J_o and IQE on L/W. This must be due to a-Si:H p-i-n device layers were deposited uniformly over the TCO.

Acknowledgments

References

[1] D. Carlson, C. Wronski, Applied Physics Letters **28**, 671 (1976).

[2] T. M. Razykov, C. S. Ferekides, D. Morel, E. Stefanakos, H. S. Ulal, H. M. Upadhyaya, Solar Energy **85**, 1580 (2011).

[3] D. L. Staebler, C. R. Wronski, Applied Physics Letters **31**, 292 (1977).

[4] S. S. Hegedus, M. Gibson, G. Ganguly, R. Arya, MRS Symp. Proc. **557**, 737 (1999).

[5] A. Alkan, R. Kaplan, H. Canbolat, S. S. Hegedus, Renewable Energy **34**, 1595 (2009).

[6] R. Kaplan, Solar Energy Materials and Solar Cells **85**, 545 (2005).

[7] J. E. Phillips, R. W. Birkmire, B. E. McCandless, P. V. Meyers, W. N. Shafarman, Phys. Stat. Sol. (b) **194**, 31 (1996).

[8] S. S. Hegedus, W. N. Shafarman, Progress in Photovoltaics: Research and Applications **12**, 155 (2004).

[9] R. Kaplan, B. Kaplan, Turkish Journal of Physics **26**, 459 (2002).

[10] S. S. Hegedus, R. Kaplan, G. Ganguly, G. Wood,

Proceedings of the 28th IEEE Photovoltaic Specialists Conference, 728 (2000).

[11] F. Zhang, X. Xu, W. Tang, J. Zhang, Z. Zhuo, J. Wang, J. Wang, Z. Xu, Y. Wang, Solar Energy Materials and Solar Cells **95**, 1785 (2011).

[12] R. Kaplan, B. Kaplan, Turkish Journal of Physics **25**, 375 (2001).

[13] B. Kaplan, Physica B: Condensed Matter **351**, 90 (2004).

[14] R. Crandal, Journal of Applied Physics **54**, 7176 (1983).

[15] S. S. Hegedus, R. Kaplan, Progress in Photovoltaics: Research and Applications **10**, 257 (2002).

[16] V. Dalal, A. Rothwarf, Journal of Applied Physics **50**, 2980 (1979).

[17] S. S. Hegedus, H. Lin, A. Moore, Journal of Applied Physics **64**, 1215 (1988).

[18] P. Chatterjee, P. McElhenry, S. Fonash, Journal of Applied Physics **67**, 3803 (1990).

_____

*Corresponding author: ruhikaplan@yahoo.com